Electronic Supplementary Material (ESI) for Catalysis Science & Technology.

Catalytic combustion of CH_2Cl_2 over SO_4^{2-}-Ti_xSn_{1-x} modified with Ru

Jian Zhao, Chensheng Tu, Wei Sun, Hangqi Xia, Hao Zhang, Qiguang Dai*, Xingyi Wang*

Research Institute of Industrial Catalysis, School of Chemistry and Molecular Engineering, East China University of Science and Technology, Shanghai 200237, PR China

N_2 adsorption-desorption isotherms and the pore size distributions

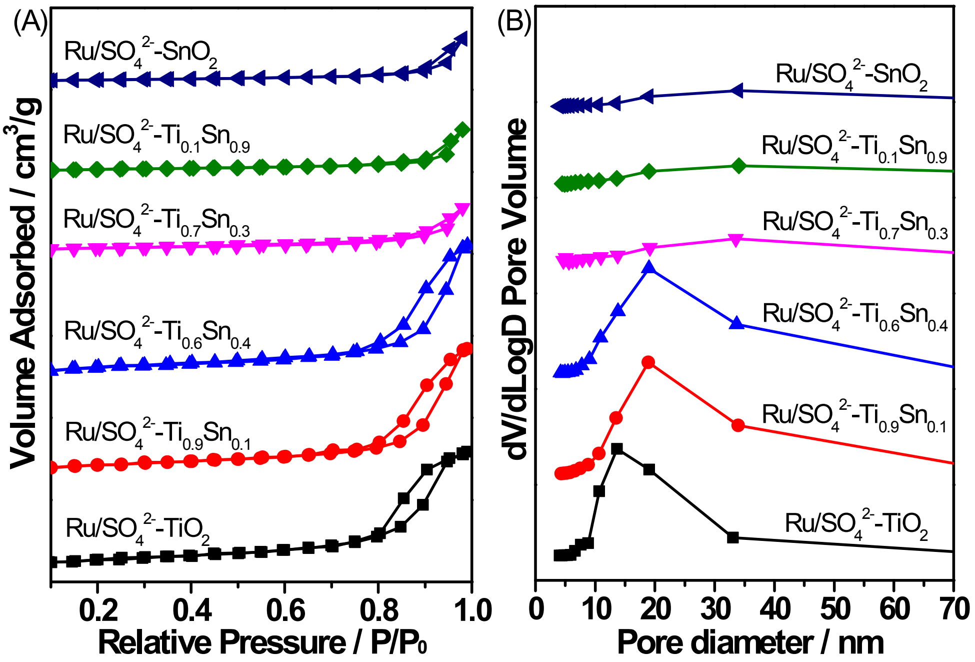

Figure S1. N_2 adsorption-desorption isotherms (A) and the pore size distributions (B) of Ru/SO_4^{2-}-Ti_xSn_{1-x} samples.

The calculated total acid amount of Ru/SO_4^{2-}-Ti_xSn_{1-x} samples

Table S1 The calculated total acid amount of Ru/SO_4^{2-}-Ti_xSn_{1-x} samples

Samples	Ti/Ti+Sn[a]	Ru/Ti_xSn_{1-x} contribution[b] / umol/m^2	S density / umol/m^2	Ti^{4+}-SO_4^{2-} contribution / umol/m^2	Total acid amount / umol/m^2
Ru/SO_4^{2-}-TiO_2	1	1.61	2.9	2.90	4.51
Ru/SO_4^{2-}-$Ti_{0.9}Sn_{0.1}$	0.90	1.80	5.7	4.90	6.70
Ru/SO_4^{2-}-$Ti_{0.6}Sn_{0.4}$	0.61	2.44	7.8	4.29	6.73
Ru/SO_4^{2-}-$Ti_{0.3}Sn_{0.7}$	0.29	2.48	9.9	3.36	5.84
Ru/SO_4^{2-}-$Ti_{0.1}Sn_{0.9}$	0.11	2.59	6.9	1.17	3.76
Ru/SO_4^{2-}-SnO_2	0	3.25	5.0	0	3.25

[a] Determined by XRF; [b]estimated by NH_3 desorption within 70–450 °C.

Total acid amount is calculated based on total acid amount of S-free (Ru/Ti_xSn_{1-x}) samples plus the amount of sulfur atom with the assumption of one acidic site per Ti^{4+}-SO_4^{2-} complex.

Ti^{4+}-SO_4^{2-} contribution = S density × Ti/Ti+Sn (Table 2)

For example

For Ru/SO_4^{2-}-$Ti_{0.6}Sn_{0.4}$:

Total acid amount = Ru/Ti_xSn_{1-x} contribution + Ti^{4+}-SO_4^{2-} contribution = 2.44 + 7.8 × 0.55 = 6.73 umol/m^2

For Ru/SO_4^{2-}-$Ti_{0.1}Sn_{0.9}$:

Total acid amount = Ru/Ti_xSn_{1-x} contribution + Ti^{4+}-SO_4^{2-} contribution = 2.59 + 6.9 × 0.17 = 3.76 umol/m^2

H_2-TPR profiles of Ru/Ti_xSn_{1-x} samples

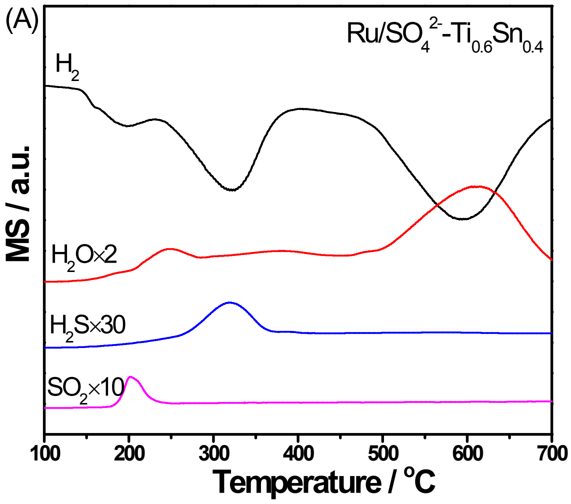

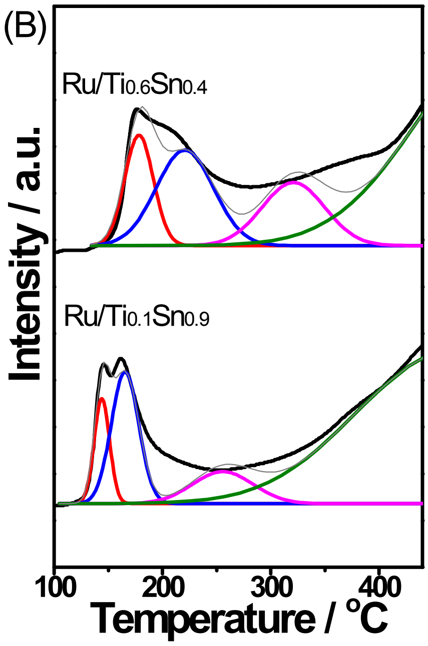

Figure S2. Products evolution over the Ru/SO_4^{2-}-$Ti_{0.6}Sn_{0.4}$ catalyst during H_2-TPR that recorded by mass spectrometry (A) and H_2-TPR profiles of Ru/Ti_xSn_{1-x} samples (B).

The calculation of H_2 consumption

The theoretical H_2 consumption of $Ru^{4+} \rightarrow Ru^0$ = n(Ru) (Table 1) × Ru^{4+}% (Table 2) × 2
The theoretical H_2 consumption of $SO_4^{2-} \rightarrow SO_2$ = n(Ru-SO_4^{2-}) × 1
The theoretical H_2 consumption of $SO_4^{2-} \rightarrow S^{2-}$ = (n(SO_4^{2-}) - n(Ru-SO_4^{2-})) × 4

For example

For Ru/SO_4^{2-}-$Ti_{0.6}Sn_{0.4}$:

The theoretical H_2 consumption of $Ru^{4+} \rightarrow Ru^0$ = $(0.93 \times 10^{-2} \times 0.54/ 101) \times 2 \times 10^{-3} = 0.099$ mmol/g

The theoretical H_2 consumption of $SO_4^{2-} \rightarrow SO_2$ = $(0.93 \times 10^{-2} / 101) \times 1 \times 10^{-3} = 0.092$ mmol/g

The theoretical H_2 consumption of $SO_4^{2-} \rightarrow S^{2-}$ = $(1.65 \times 10^{-2} / 32 - 0.93 \times 10^{-2} / 101) \times 4 \times 10^{-3} =$

1.694 mmol/g

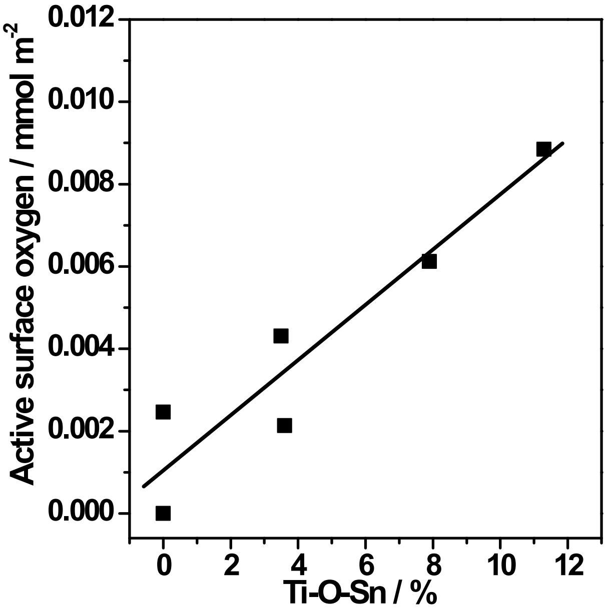

Figure S3. Active surface oxygen *vs* the content of Ti-O-Sn of Ru/SO_4^{2-}-Ti_xSn_{1-x} samples.

Activity of SO_4^{2-}-Ti_xSn_{1-x} catalysts for CH_2Cl_2 combustion

Table S2 Activity of SO_4^{2-}-Ti_xSn_{1-x} catalysts for CH_2Cl_2 combustion

Sample	T_{50} / °C	T_{90} / °C	Ea / KJ / mol	TOF_S ^{a}×10^{-3} / s^{-1}
SO_4^{2-}-TiO_2	255	372	65	0.02
SO_4^{2-}-$Ti_{0.9}Sn_{0.1}$	225	269	62	0.27
SO_4^{2-}-$Ti_{0.6}Sn_{0.4}$	216	257	52	0.28
SO_4^{2-}-$Ti_{0.3}Sn_{0.7}$	254	314	57	0.21
SO_4^{2-}-$Ti_{0.1}Sn_{0.9}$	300	372	63	0.18
SO_4^{2-}-SnO_2	400	461	81	0.02

[a] based on conversions at 225 °C in Figure 7.

Calculation of Rate and TOF_S

Rate at 225 °C based on the converted mole number of CH_2Cl_2 and at 225 °C per second per square shown in Table 4.

TOF_S calculated based on net increase in the rates due to Ti^{4+}-SO_4^{2-} normalized by the corresponding sulfur content.

Reaction condition: feed: 100 mL/min; 1000 ppm CH_2Cl_2, 10% O_2 and N_2 in balance; catalyst: 200 mg.

For example

For Ru/SO_4^{2-}-$Ti_{0.6}Sn_{0.4}$:
CH_2Cl_2 conversion at 225°C: 72.0%;
S density: 7.8 umol/m^2;
S_{BET}: 66 m^2/g
Ru/$Ti_{0.1}Sn_{0.9}$:
CH_2Cl_2 conversion at 225°C: 18%; S_{BET}: 55 m^2/g.

Rate = CH_2Cl_2 concentration × feed × conversion / (22.4 × m_{cat} × S_{BET}) = $1000\times 100 \times 10^{-3} \times 72.0 \times 10^{-2} / (22.4 \times 0.2 \times 66) = 0.24$ umol/min m^2

TOF_S = net increase in rate normalized by Ti^{4+}-SO_4^{2-}
= 1000 ppm × 10^{-6} (CH_2Cl_2 concentration) ×100 ml/min (feed) ×10^{-3}× (72/66-18/55) / (22.4 × 0.2g (m_{cat})×7.8 umol/m^2 (S density) × 0.55(Ti/Ti+Sn)×10^{-6}× 60 second)=0.63×10^{-3} s^{-1}

Stability test

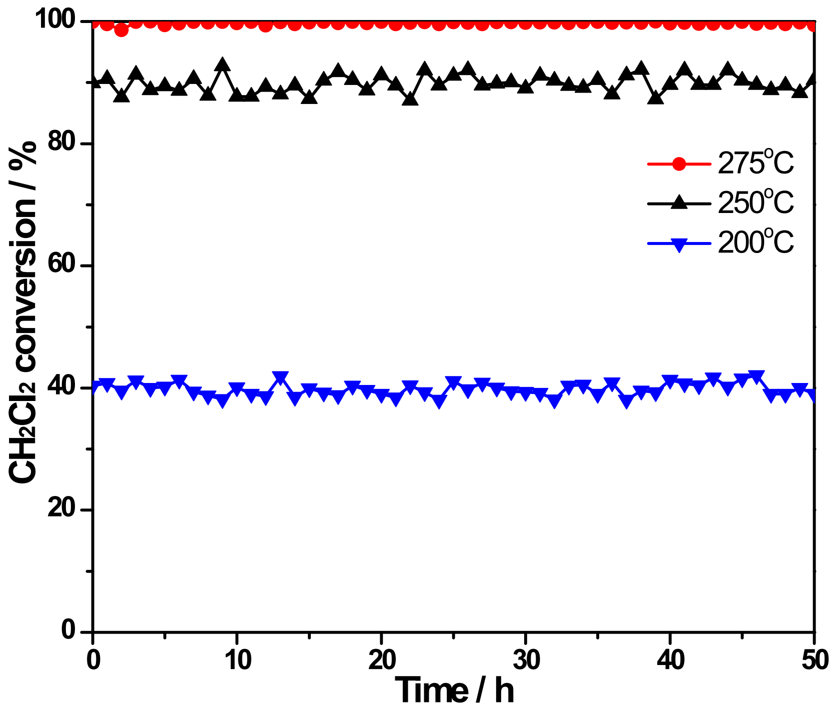

Figure S4. The stability of Ru/SO_4^{2-}-$Ti_{0.6}Sn_{0.4}$ on CH_2Cl_2 stream at various temperatures; gas composition: 1000 ppm CH_2Cl_2, 10% O_2 and N_2 balance; GHSV = 30,000 mL g^{-1} h^{-1}; catalyst amount: 200 mg.

The effect of S loading on CH_2Cl_2 oxidation

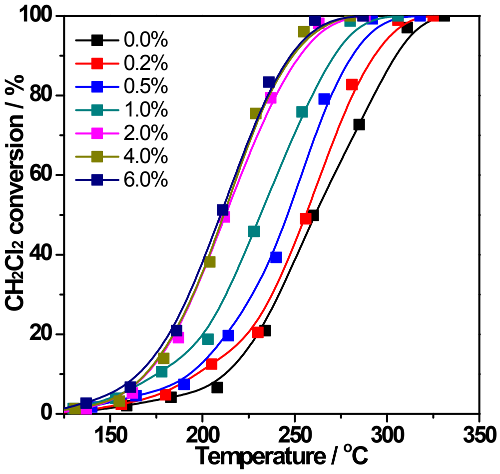

Figure S5. CH_2Cl_2 conversion curves of various S loadings over Ru/SO_4^{2-}-$Ti_{0.6}Sn_{0.4}$; gas composition: 1000 ppm CH_2Cl_2, 10% O_2 and N_2 balance; GHSV = 30,000 mL g^{-1} h^{-1}; catalyst amount: 200 mg.

The effect of O_2 concentration on CH_2Cl_2 oxidation

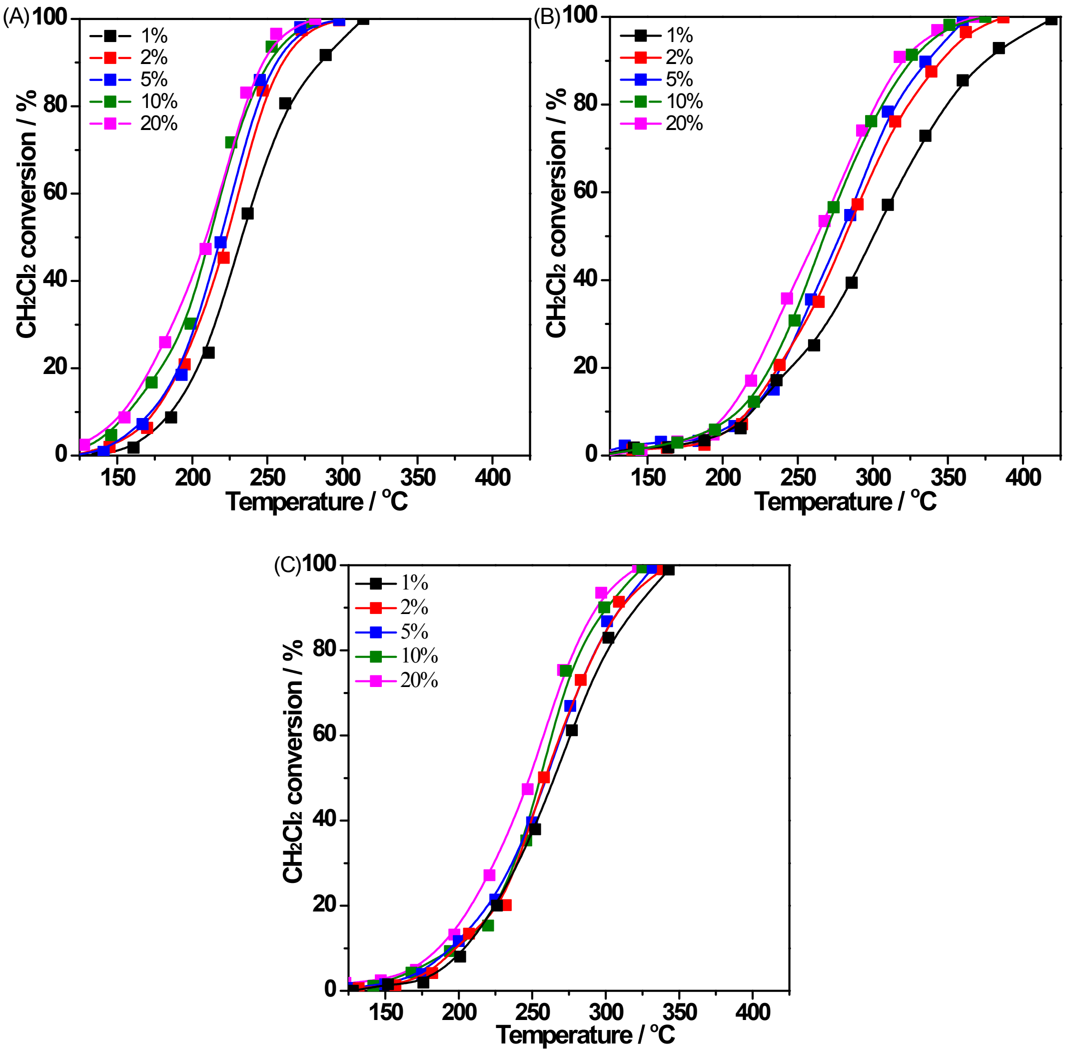

Figure S6. The effect of inlet O_2 concentration on CH_2Cl_2 oxidation over Ru/SO_4^{2-}-$Ti_{0.6}Sn_{0.4}$ (A), Ru/SO_4^{2-}-$Ti_{0.1}Sn_{0.9}$ (B) and Ru/$Ti_{0.6}Sn_{0.4}$ (C); gas composition: 1000 ppm CH_2Cl_2, 1-20% O_2 and N_2 balance; GHSV = 30,000 mL g^{-1} h^{-1}; catalyst amount: 200 mg.

The effect of CH_2Cl_2 concentration on CH_2Cl_2 oxidation

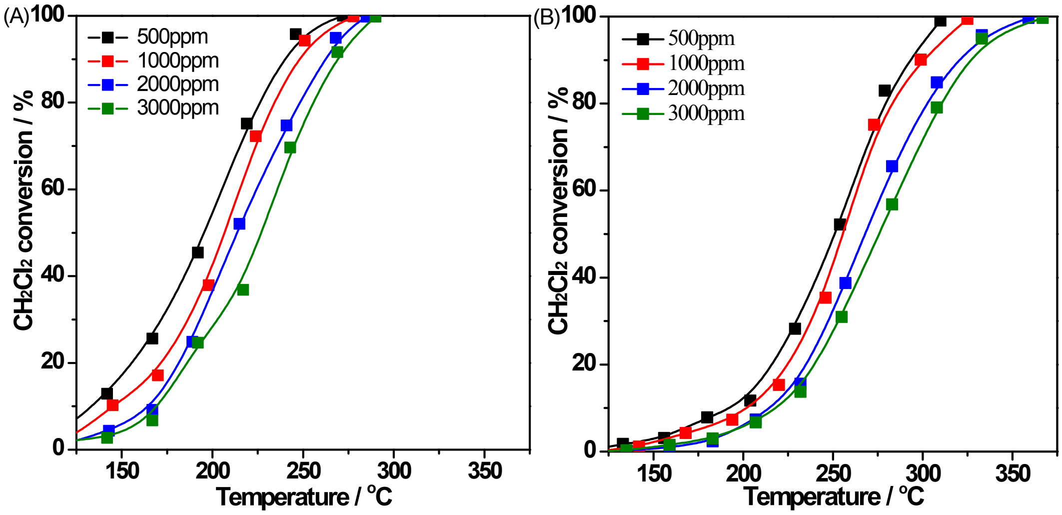

Figure S7. The effect of inlet CH_2Cl_2 concentration on CH_2Cl_2 oxidation over Ru/SO_4^{2-}- $Ti_{0.6}Sn_{0.4}$ (A) and Ru/$Ti_{0.6}Sn_{0.4}$ (B); gas composition: 500–3000 ppm CH_2Cl_2, 10% O_2 and N_2 balance; GHSV = 30,000 mL g^{-1} h^{-1}; catalyst amount: 200 mg.

Apparent activation energy

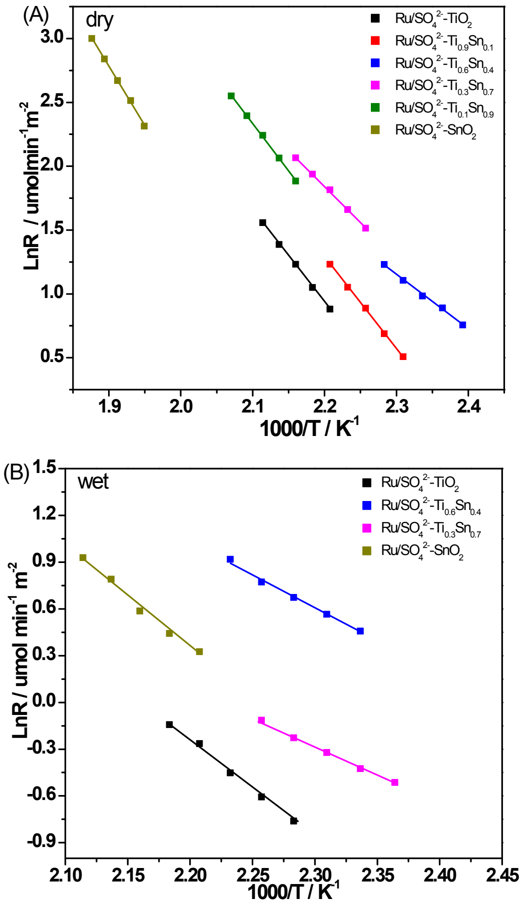

Figure S8. Arrhenius plots for CH_2Cl_2 oxidation in dry (A) and wet feed (2% H_2O) (B) over Ru/SO_4^{2-}-Ti_xSn_{1-x} catalysts; gas composition: 1000 ppm CH_2Cl_2, 10% O_2 and N_2 balance; GHSV: 30,000 mL g^{-1} h^{-1}; catalyst amount: 200 mg.

TPSR

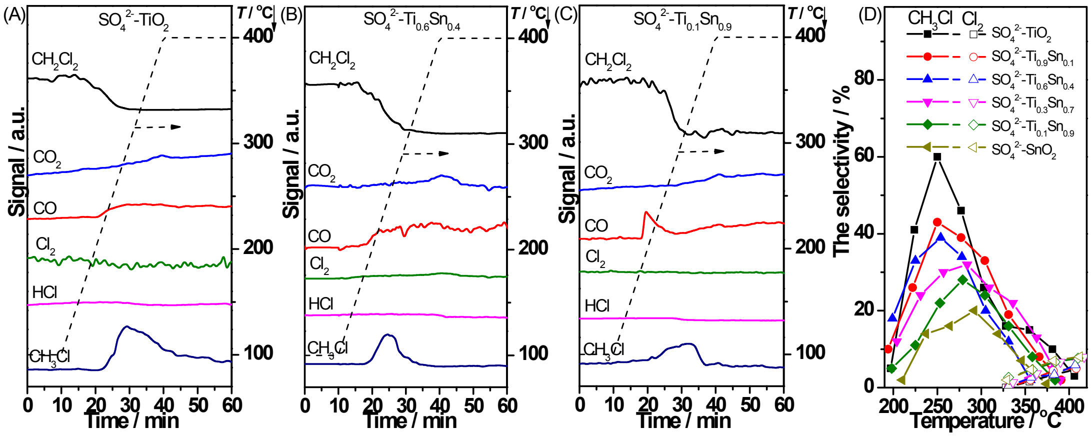

Figure S9. The product distributions during TPSR experiments of SO_4^{2-}-TiO_2 (A), SO_4^{2-}-$Ti_{0.6}Sn_{0.4}$ (B) and SO_4^{2-}-$Ti_{0.1}Sn_{0.9}$ (C), and the selectivity of CH_3Cl and Cl_2 over SO_4^{2-}-Ti_xSn_{1-x} (D) catalysts; gas composition: 1000 ppm CH_2Cl_2, 10% O_2 and N_2 balance; GHSV = 30,000 mL g^{-1} h^{-1}; catalyst amount: 200 mg.

FT-IR spectra of spent Ru/SO_4^{2-}-Ti_xSn_{1-x} catalysts in wet feed

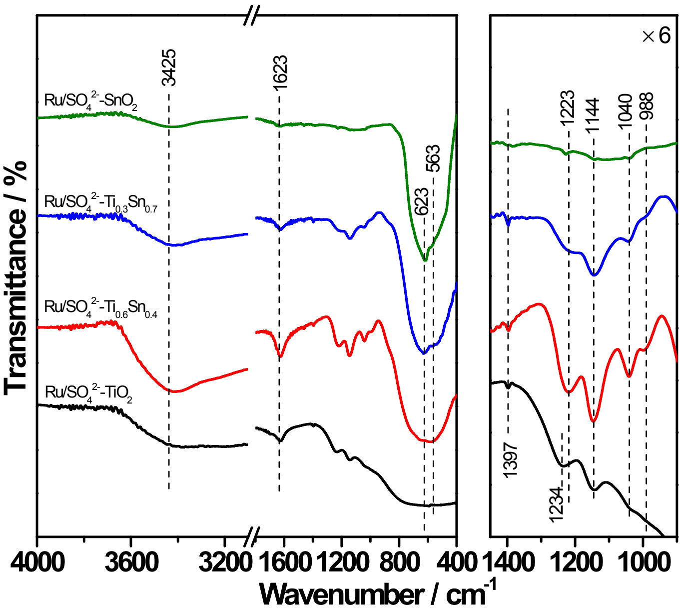

Figure S10. FT-IR spectra of spent Ru/SO_4^{2-}-Ti_xSn_{1-x} samples in wet feed (2% H_2O).

Characterization for spent Ru/SO$_4^{2-}$-Ti$_x$Sn$_{1-x}$catalysts

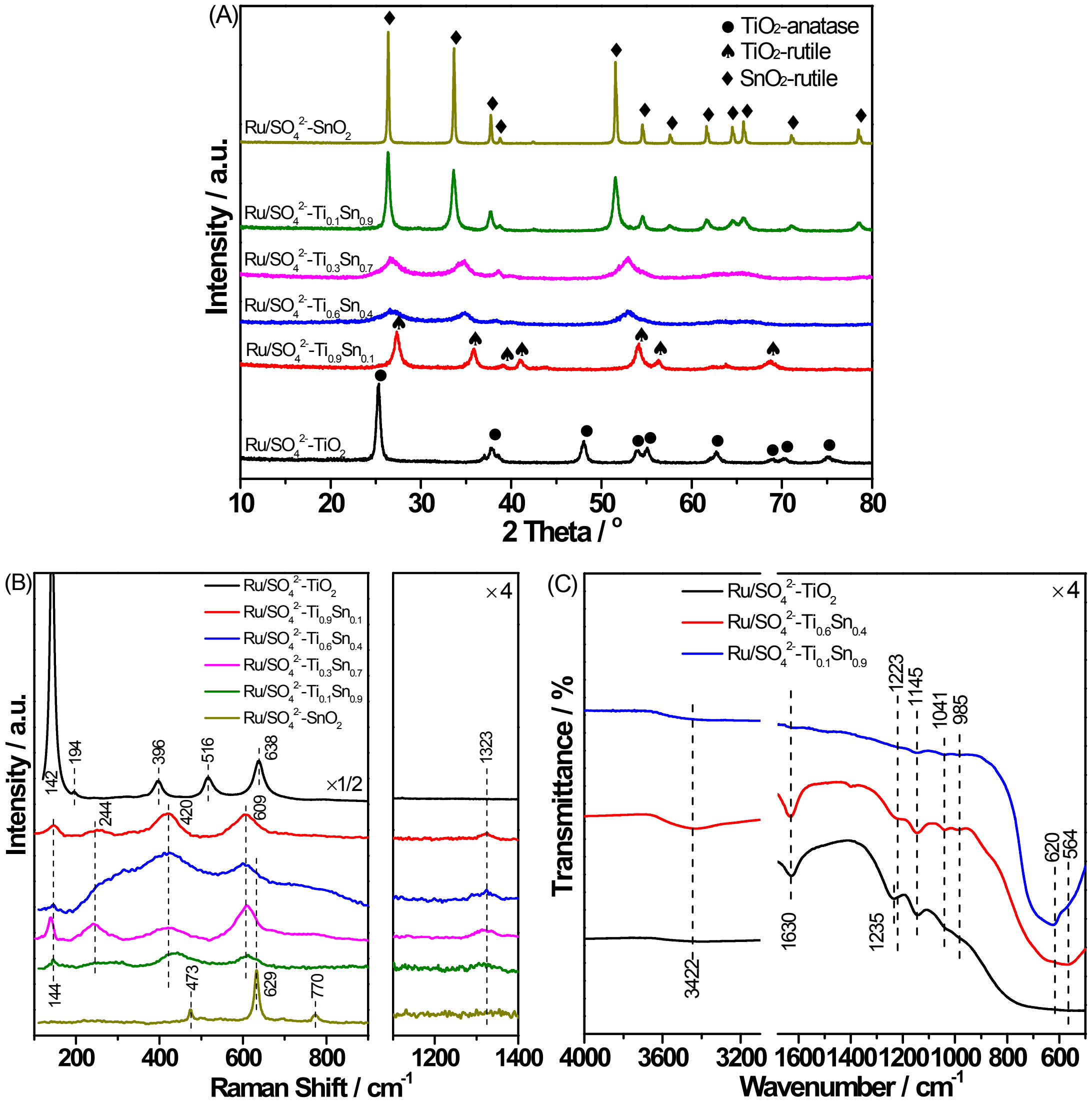

Figure S11. XRD (A), Raman (B) and FT-IR (C) spectra of spent Ru/SO$_4^{2-}$-Ti$_x$Sn$_{1-x}$ samples.

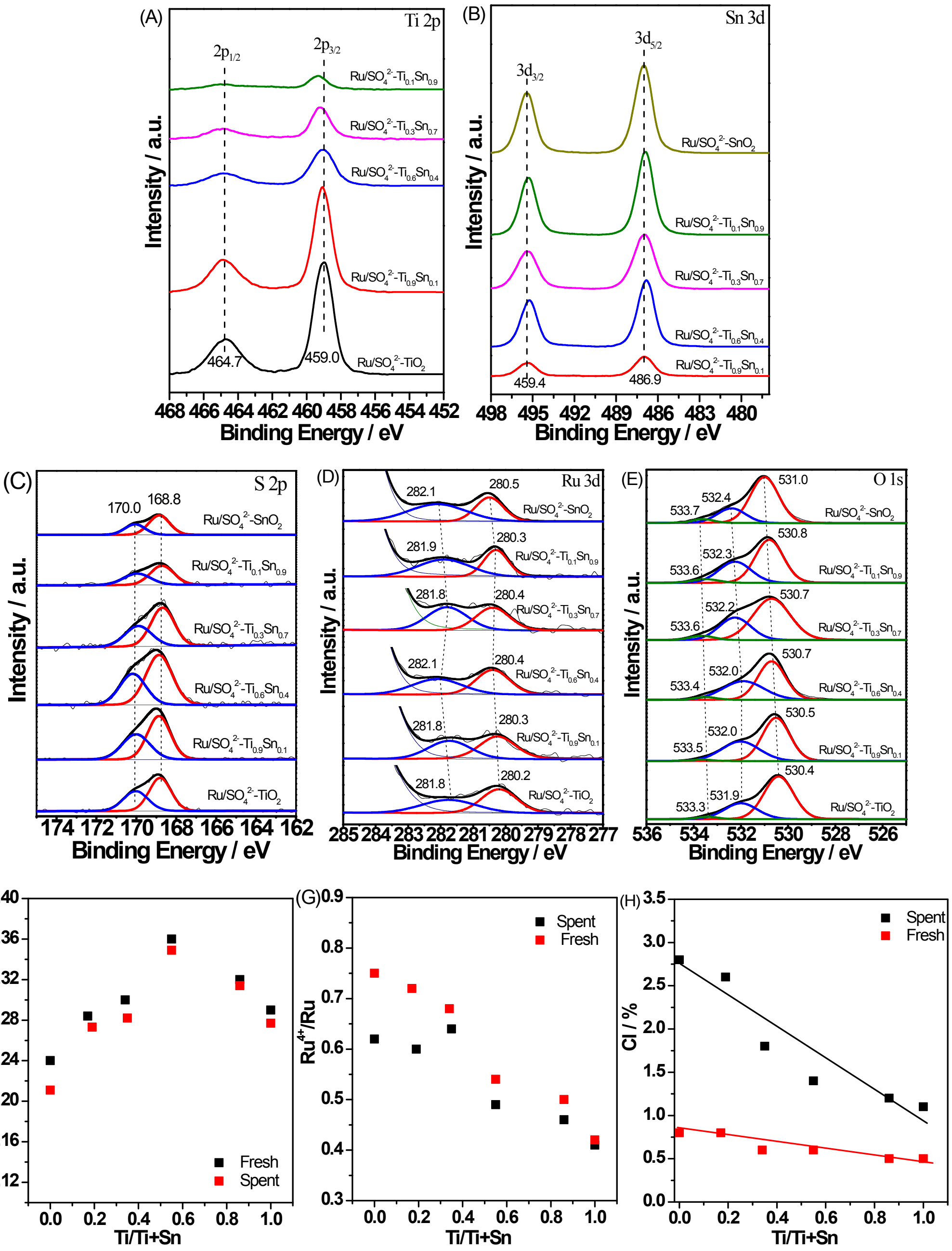

Figure S12. XPS spectra of Ti 2p (A), Sn 3d (B), S 2p (C), Ru 3d (D) and O 1s (E), and O_{sur}/O_{total} (F), Ru^{4+}/Ru (G) and Cl content *vs* Ti/Ti+Sn (H) of spent Ru/SO_4^{2-}-Ti_xSn_{1-x} samples.

H_2-TPR profiles of spent Ru/SO_4^{2-}-Ti_xSn_{1-x} catalysts

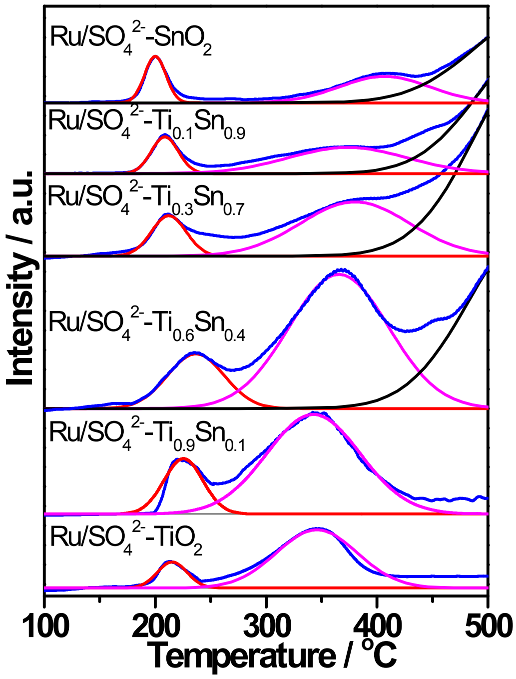

Figure S13. H_2-TPR profiles of spent Ru/SO_4^{2-}-Ti_xSn_{1-x} samples.

Table S3 H_2-TPR results of spent Ru/SO_4^{2-}-Ti_xSn_{1-x} samples

Sample	H_2 uptake at the first peak / mmol/g				H_2 uptake at the second peak / mmol/g		
	$Ru^{4+}\rightarrow Ru^0$	$SO_4^{2-}\rightarrow SO_2$	O_{sur}[a]	Total	$SO_4^{2-}\rightarrow S^{2-}$	Surface Sn	Total
Ru/SO_4^{2-}-TiO_2	0.076	0.090	---	0.157	0.665	0.567(0.00659)(O_{sur})	1.232
Ru/SO_4^{2-}-$Ti_{0.9}Sn_{0.1}$	0.089	0.089	0.416(0.00533)	0.594	1.421	0.400(0.00578) (O_{sur})	1.872
Ru/SO_4^{2-}-$Ti_{06}Sn_{0.4}$	0.099	0.092	0.545(0.00826)	0.736	1.694	0.220	1.914
Ru/SO_4^{2-}-$Ti_{0.3}Sn_{0.7}$	0.120	0.088	0.209(0.00746)	0.417	0.761	0.407	1.168
Ru/SO_4^{2-}-$Ti_{0.1}Sn_{0.9}$	0.134	0.093	0.069(0.00363)	0.296	0.153	0.558	0.711
Ru/SO_4^{2-}-SnO_2	0.138	0.078	0.061(0.00406)	0.277	---	0.501	0.501

[a] The values within bracket, O_{sur} density, mmol/m^2.